

Higher-Order Topological Insulators with Fractional Charges Modulated by Lorentz Transformation

Yuwei Hu¹, Suge Feng¹, Boquan Ren¹, Hua Zhong¹, Milivoj R. Belić²,
Meng Cao¹, Yongdong Li¹, Tao Wang³, Yiqi Zhang¹✉

(1. Key Laboratory for Physical Electronics and Devices, Ministry of Education, School of Electronic Science and Engineering, Xi'an Jiaotong University, Xi'an 710049, China;
2. College of Science and Engineering, Hamad Bin Khalifa University, 23874 Doha, Qatar; 3. Grace Laser, Beijing 101318, China)

Abstract: Topological insulators represent a new phase of matter, characterized by conductive surfaces, while their bulk remains insulating. When the dimension of the system exceeds that of the topological state by at least two, the insulators are classified as higher-order topological insulators (HOTI). The appearance of higher-order topological states, such as corner states, can be explained by the filling anomaly, which leads to the fractional spectral charges in the unit cell. Previously reported fractional charges have been quite limited in number and size. In this work, based on the two-dimensional (2D) Su-Schrieffer-Heeger model lattice, we demonstrated a new class of HOTIs with adjustable fractional charges that can take any value ranging from 0 to 1, achieved by utilizing the Lorentz transformation. Furthermore, this transformation generates novel bound-state-in-continuum-like corner states, even when the lattice is in a topological trivial phase, offering a new approach to light beam localization. This work paves the way for fabricating HOTIs with diverse corner states that offer promising applicative potential.

Keywords: topological insulator; corner state; spectral charge; Lorentz transformation

1 Introduction

Higher-order topological insulators (HOTIs) are a special class of topological insulators whose dimension is lower than that of the system by no less than two [1–5]. Generally, HOTIs can be divided into two categories: those characterized by nonzero quantized multipole moments [6–11], and those without such moments [12–26]. HOTIs realized in classical wave platforms, such as pho-

tonic systems, mostly belong to the latter category. However, photonic HOTIs belonging to the first category were also reported recently, achieved by properly manipulating the coupling strengths among lattice sites [11, 27, 28].

It has been shown that the emergence of topological states (for example, corner states) is a result of the “filling anomaly”, which induces fractional charges [6, 12, 29, 30]. In classical wave platforms, the term “charge” refers to the spectral charge, which represents the number of states within a unit cell, taking into account all states below the topological states [31, 32]. The charge in a unit cell can be determined using the Wannier center method [33]. It is worth noting that the topological states in photonic HOTIs have been reported in various experiments,

Manuscript received Sep. 30, 2024; revised Jan. 18, 2025; accepted Feb. 4, 2025. The associate editor coordinating the review of this manuscript was Dr. Nan Zhang. The work was supported by the Natural Science Basic Research Program of Shaanxi Province (No. 2024JC-JCQN-06), the National Natural Science Foundation of China (Nos. 12474337, 12304370), and Fundamental Research Funds for the Central Universities (No. zxy012024135).

✉ Corresponding author. Email: zhangyiqi@xjtu.edu.cn
DOI: 10.15918/j.jbit1004-0579.2024.097

including both periodic [15, 16, 25, 34, 35] and aperiodic lattices [24, 26, 30].

Even though the appearance of corner states has been well explained by fractional charges, the range of fractional charge values reported so far has been quite limited [12]. For instance, in a two-dimensional (2D) Su-Schrieffer-Heeger (SSH) model lattice, the fractional charge for corner states is typically 1/4. Similarly, the value is 1/3 in the Kagome lattice and 2/3 in the honeycomb lattice. Clearly, these fractional charges are quite limited in their number and cannot be expanded [12], to the best of our knowledge. Whether these fractional charge values can be manipulated and how to reach this goal, so that fractional charges can be manipulated in both number and size, is an intriguing question worth exploring.

Taking the 2D SSH model lattice as an example, the corner unit cell only contains a quarter of the Wannier center, and hence the corner charge is 1/4. From this point of view, if one can adjust the corner angle, then the ratio of the Wannier center occupied by the corner unit cell can be changed. Considering that Lorentz transformation [36] deforms coordinates, we introduced it in this work to distort the lattice geometry and modify its structure. As a result, we obtained topological corner states with arbitrary fractional charges distributed in the range (0, 1). In addition, after Lorentz transformation we also obtained localized corner states, even when the lattice is, for example, in a topological trivial phase.

2 Theoretical Model

The propagation dynamics of the light beam in a photonic lattice can be described by a Schrödinger-like paraxial wave equation

$$i \frac{\partial \psi}{\partial z} = -\frac{1}{2} \left(\frac{\partial^2}{\partial x^2} + \frac{\partial^2}{\partial y^2} \right) \psi - \mathcal{R}(x, y) \psi \quad (1)$$

where ψ is the dimensionless complex amplitude of the light field, and x , y and z are the normalized transverse coordinates and the propagation

distance, respectively. The function below describes the photonic lattice waveguide, shown as

$$\mathcal{R}(x, y) = p \sum_{mn} e^{-(x-x_m)^2/d^2 - (y-y_n)^2/d^2} \quad (2)$$

The function describes the photonic lattice waveguide with the depth p and width d placed at the nodes (x_m, y_n) of the grid. The lattice waveguide can be fabricated using the femto-second laser direct writing technique in the fused silica material [22, 24–26, 37–43] or can be induced in photorefractive crystals [44–48] and atomic ensembles [49, 50]. We assume the lattice waveguide is prepared using the first method; then the typical values of quantities in Eq. (1) are: the lattice constant $a = 1.6$ (16 μm), the waveguide width $d = 0.5$ (5 μm), and the lattice potential depth $p = 10$ (the corresponding refractive index change is $\Delta n = pn_0/k^2 r_0^2 \sim 6.3 \times 10^{-4}$), where $n_0 = 1.45$ is the ambient refractive index, $k = 2n_0\pi/\lambda$, $\lambda = 600$ nm, and $r_0 = 10$ μm . These parameter values are quite common for the first method, and the results will not be affected much if some parameters get adjusted, as illustrated in the previous literature [24–26].

In Fig. 1 (a), we depict the 2D SSH model lattice with a displayed. The quantity r is the controlling parameter that adjusts the separation distance among four sites in one unit cell.

If we introduce the Lorentz transformation [36, 51] of the lattice through

$$\begin{bmatrix} x' \\ y' \end{bmatrix} = \mathcal{M} \begin{bmatrix} x \\ y \end{bmatrix} \quad (3)$$

where

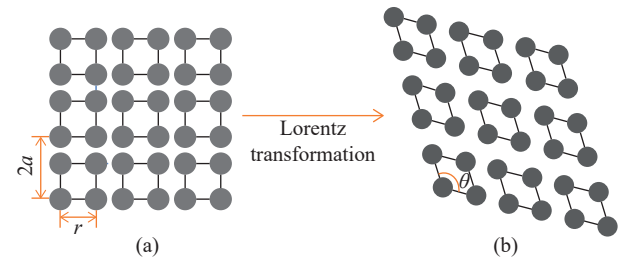


Fig. 1 Schematic diagram of the Lorentz transformation of 2D SSH lattice: (a) before transformation; (b) after transformation

$$\mathcal{M} = \begin{bmatrix} \cosh(\zeta/2) & \sinh(\zeta/2) \\ \sinh(\zeta/2) & \cosh(\zeta/2) \end{bmatrix} \quad (4)$$

with

$$\zeta = \tanh^{-1}(\cos \theta) \quad (5)$$

the 2D SSH lattice will be deformed, as shown in Fig. 1(b), in which the corner angle θ is also presented. Clearly, if $\theta = \pi/2$, the lattice is not deformed, since matrix \mathcal{M} is then an identity. If we change the grid coordinates of $\mathcal{R}(x, y)$ in Eq. (1) from (x_m, y_n) to (x'_m, y'_n) , then the lattice will be manipulated by an angle θ . For convenience, we denote the transformed lattice as $\mathcal{R}(x, y, \theta)$.

Generally, the ansatz solution of Eq. (1) can be written as $\psi(x, y, z) = u(x, y)e^{ibz}$, and plugging it into Eq. (1) one obtains

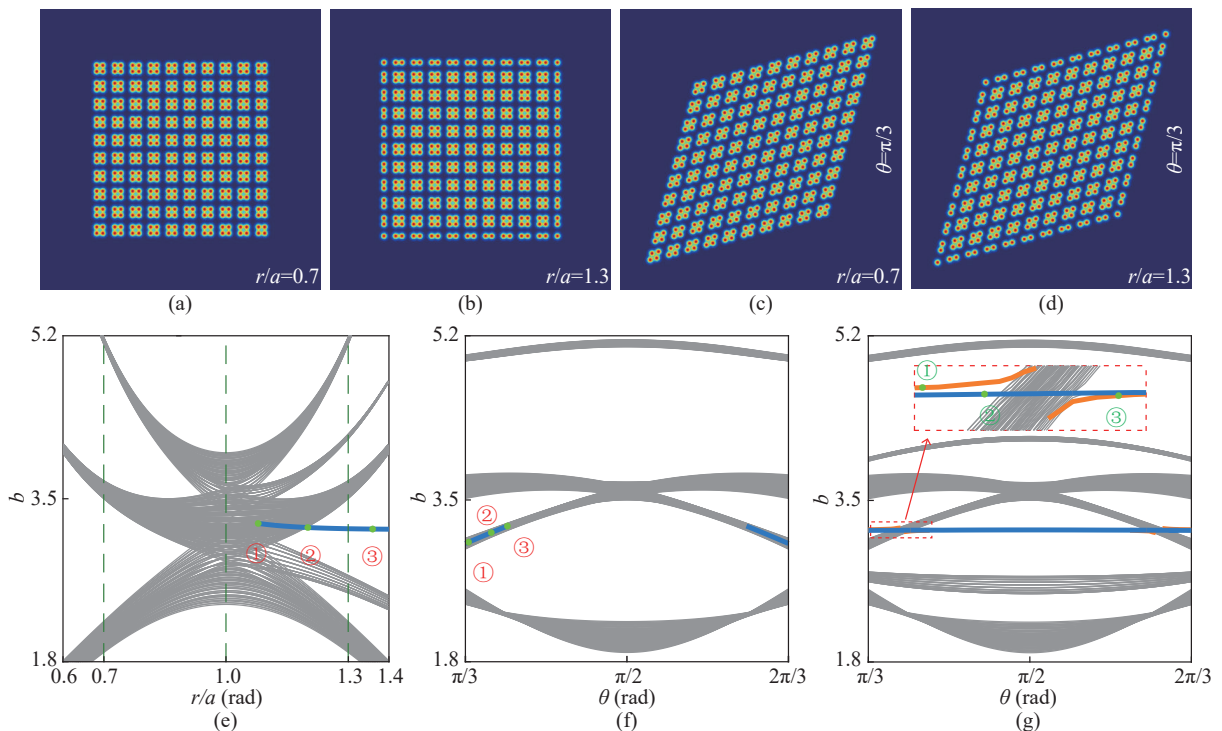
$$bu = \frac{1}{2} \left(\frac{\partial^2}{\partial x^2} + \frac{\partial^2}{\partial y^2} \right) u + \mathcal{R}(x, y, \theta)u \quad (6)$$

where $u(x, y)$ is the envelope of the light beam and b in optical applications represents the propagation constant. The eigenvalue problem in Eq. (6) can be numerically solved using the plane-wave expansion method, which gives the relation between b and r that defines the spectrum of the lattice. In the next section, we would like to discuss our results. Note that the Lorentz transformation is adopted just as a method for manipulating the lattice; there is nothing relativistic in this work. The transformation does not affect the paraxial wave equation itself, but it may affect its solutions.

3 Results

3.1 Spectra and Modes

Spectra of the 2D SSH model lattice for different values of parameters are displayed in Fig. 2. We



Note: In Fig. 2 (e), the blue line represents the corner states, while the gray lines bulk states and edge states. In Fig. 2 (f), the blue line represents the localized states, while the gray lines represent the extended states. In Fig. 2 (g), the blue and orange lines are corner states, while the gray lines bulk states and edge states.

Fig. 2 Two-dimensional SSH model lattice and the corresponding spectrum: (a) lattice with $r/a = 0.7$; (b) lattice with $r/a = 1.3$; (c) transformed lattice with $r/a = 0.7$ and $\theta = \pi/3$; (d) transformed lattice with $r/a = 1.3$ and $\theta = \pi/3$; (e) spectrum of the lattice as a function of r ; (f) spectrum of the transformed lattice with $r/a = 0.7$ as a function of θ ; (g) spectrum of the transformed 2D SSH lattice with $r/a = 1.3$ as a function of θ

examined two representative lattices, one for $r/a = 0.7$ (in the topological trivial phase) and the other for $r/a = 1.3$ (in the topological phase as well), shown in Fig. 2(a) and Fig. 2(b). The spectrum of the lattice as a function of r is shown in Fig. 2(e). The blue line in Fig. 2 indicates the corner states, and is four-fold degenerate, due to the C_4 symmetry of the lattice. To track the spectrum of the lattice after Lorentz transformation, we depicted both $r/a = 0.7$ and $r/a = 1.3$ cases, with the corresponding transformed lattices for $\theta = \pi/3$, in Fig. 2(c) and Fig. 2(d), respectively. Following the transformation, the lattice symmetry is reduced to C_2 , causing the four-fold degenerate corner states to split into two pairs of two-fold degenerated corner states (see the spectrum in Fig. 2(g)).

In Fig. 2(f), we present the spectrum of the transformed lattice with $r/a = 0.7$ as a function of θ . One cannot find any explicit state in the band gaps. However, in the bulk, there are localized states, as indicated by the blue lines, which represent bound-state-in-continuum (BIC)-like states. These BIC-like localized states do not exist in the original 2D SSH model; they are entirely novel states, arising solely due to the transformation of the lattice.

If the original 2D lattice is in the topological phase, the spectrum of the transformed lattice with $r/a = 1.3$ is shown in Fig. 2(g). One finds that the corner states, indicated by blue and orange lines, are always there, regardless of the value of θ . For clarity, the part of the spectrum enclosed by the dashed rectangle is magnified and displayed as an inset. This reveals that the four four-fold degenerate corner states split into two pairs of two-fold degenerate corner states, as indicated by the blue and orange lines. Similar to the case in the topological trivial phase, the two overlapping bulk bands at $\theta = \pi/2$ separate as θ deviates from $\theta = \pi/2$. Since the corner states hybridize with the separated bulk bands, only the corner states associated with the obtuse angle (indicated by the orange line) are

clearly visible. On the other hand, the blue corner states that appear at the acute angle can cross the separated gray bulk band as the angle θ changes.

We selected three localized states from Fig. 2(e), Fig. 2(f), and Fig. 2(g), marked by green dots numbered 1, 2, and 3, and presented their field modulus profiles in Fig. 3. The corner states from the original undeformed 2D SSH lattice are shown in Fig. 3(a), which align well with the previous findings [47, 52]. For the BIC-like corner states depicted in Fig. 3(b), it is evident that the closer the angle θ to $\pi/2$, the worse the localization of the state. Nonetheless, these BIC-like corner states do exist in the deformed 2D SSH model lattice, even when the lattice is in the topological trivial phase. When the deformed lattice is in the topological phase, the selected corner states, derived from a different pair of corner states, are shown in Fig. 3(c). States numbered 1 and 3 from the orange lines are localized at corners with the obtuse angle, while state 2 from the blue line is localized at corners with the acute angle. Thus far, we have demonstrated that the Lorentz transformation effectively manipulates both the appearance and the profile of the corner states.

3.2 Wannier Centers

Next, we examined the Wannier centers of the lattice for different values of parameters. The Wannier center refers to the position of the center of Wannier functions. The wave functions describing the states. It is positioned relative to the strong bonds of atoms, i.e. to the sites of the lattice. The Wannier center may be located in the corner of the unit cell or in the middle of the boundary between two unit cells, if the lattice is in the crystalline topological phase. In the topological trivial phase, the Wannier centers are in the middle of unit cells. In our case, the Wannier centers are in the corners of unit cells if the lattice is in the crystalline topological phase, as shown in Fig. 4. From the Wannier centers, the

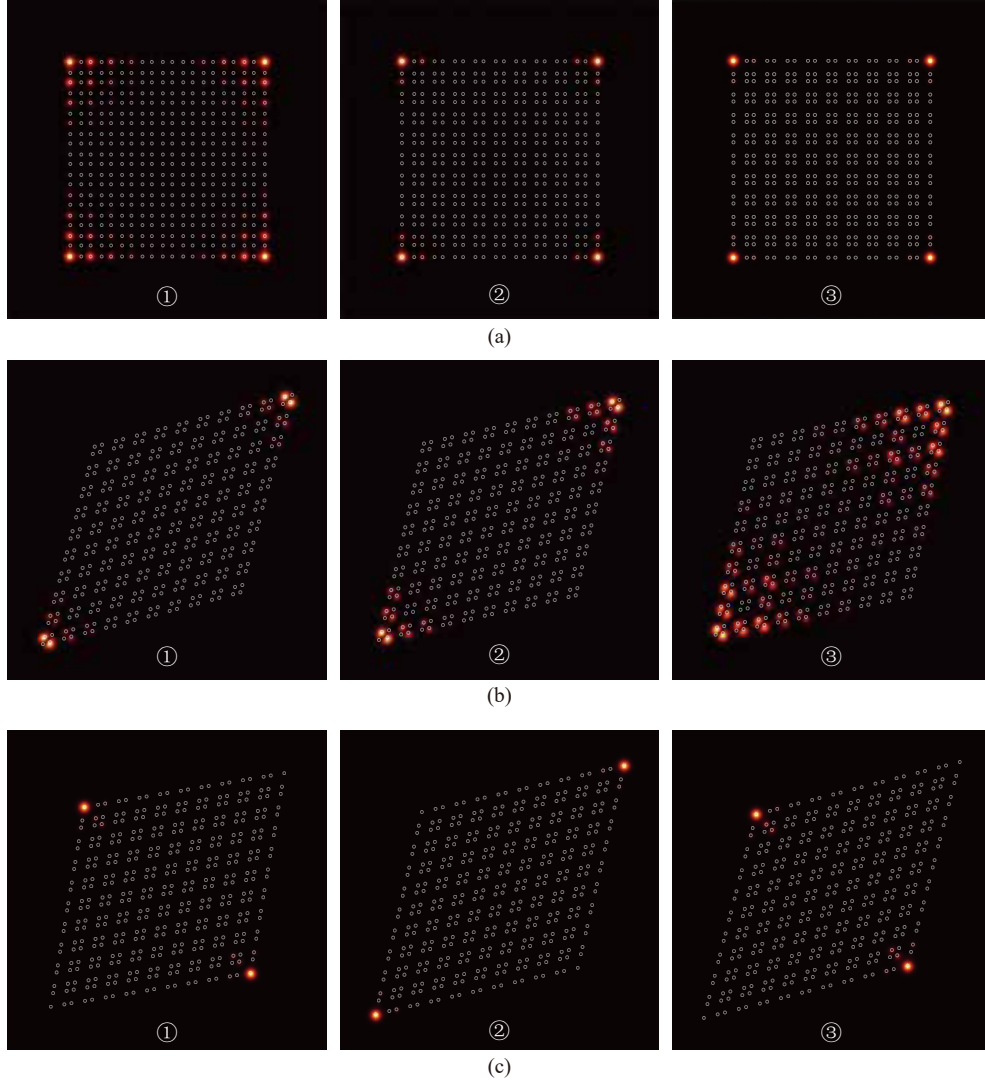


Fig. 3 Field modulus profiles of the corner states: (a) corresponding to numbered dots in Fig. 2(e); (b) same as (a) but for the dots in Fig. 2(f); (c) same as (b) but for the dots in Fig. 2(g)

fractional charge of each unit cell can be easily predicted [12, 29, 30].

Fig. 4(a) and Fig. 4(b), depict the Wannier centers (red dots) of the undeformed 2D SSH model, corresponding to the topological trivial phase and the topological phase, respectively. The two cases are well established: in the topological trivial phase the Wannier centers are located at the center of the unit cell, while in the topological phase they shift to the corner grid point of the unit cell. Since the corner unit cell holds $1/4$ of the spectral charge and the edge unit cell holds $1/2$ of the spectral charge, as shown in Fig. 4(b), one can anticipate the presence of both corner and edge states in the final

count [3].

When the lattice is deformed using the Lorentz transformation, the Wannier centers remain at the center of the unit cell, if the lattice is in the topological trivial phase, as shown in Fig. 4(c). In this case, there is no fractional spectral charge in any of the unit cells. However, as demonstrated in Fig. 2 and Fig. 3, the localized corner states still exist. These states are not topological objects but resemble BIC. If the deformed lattice is in the topological phase, as shown in Fig. 4(d) with a deformation angle of $\theta = 2\pi/3$, the Wannier center occupied by the corner unit cells is not $1/4$ any more. For instance, the upper-left corner unit cell occupies

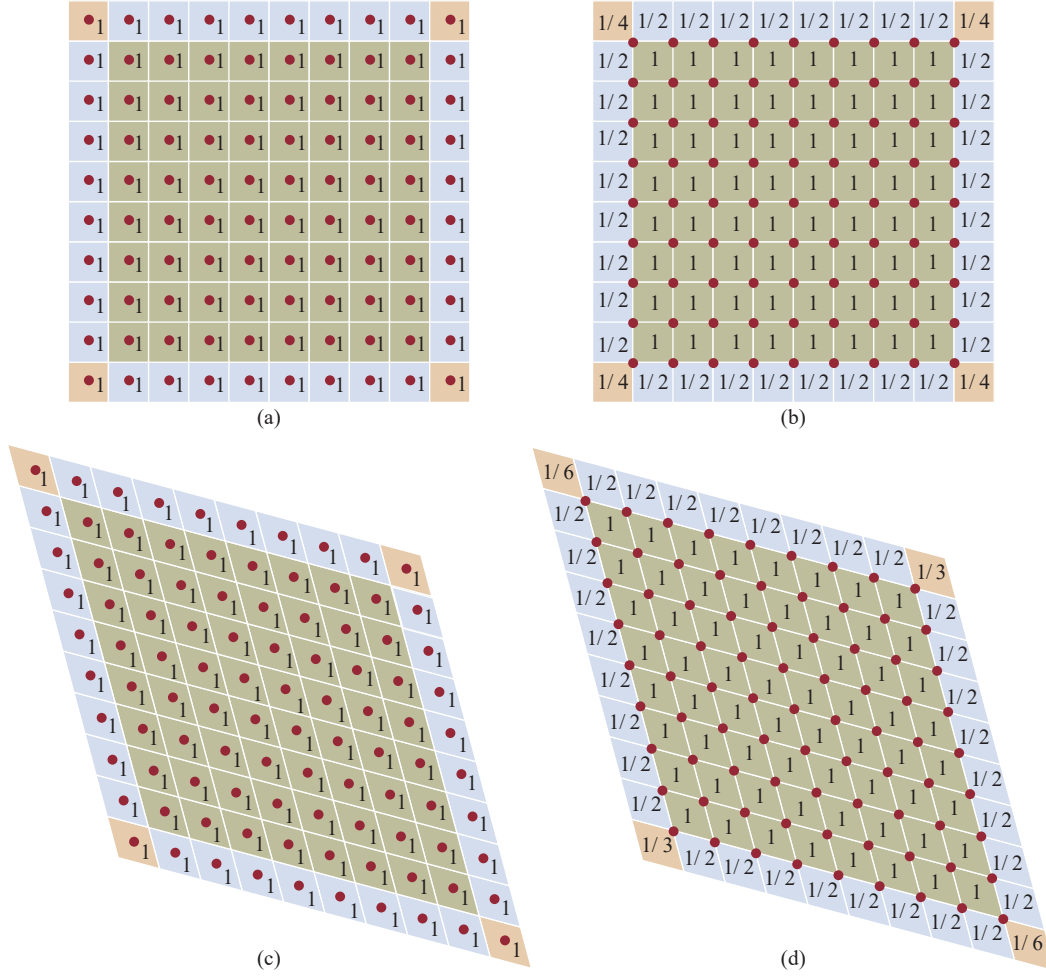


Fig. 4 Wannier centers: (a) Wannier center (red dots) in the topological trivial 2D SSH lattice; (b) setup is as (a) but in topological phase; (c), (d) setup is as (a), (b) but for deformed lattice with $\theta = 2\pi/3$

only $1/6$ of the Wannier center on the grid, giving it a fractional charge of $1/6$. The bottom-left corner unit cell has a fractional charge of $1/3$. In general, the fractional charge ϱ for the corner unit cell is determined from the angle θ via the relation

$$\varrho = \frac{\theta}{2\pi} \quad (7)$$

This formula is quite reasonable. A Wannier center brings a charge of 1, and it is shared by 4 unit cells if the lattice is in the crystalline topological phase. Therefore, the charge 1 should be divided into 4 parts, and the portion obtained for each unit cell is determined by the angle of the unit cell. As the charge of 1 corresponds to 2π , the fractional charge acquired by one unit cell is $\theta/2\pi$. Since angle θ can be arbitrarily chosen in

the range $(0, 2\pi)$, the fractional charge of the corner unit cell can acquire an arbitrary fractional value. For the total count, one should keep in mind that the fractional charge of the edge of the unit cell is always $1/2$.

4 Conclusion

In summary, we have introduced a new class of HOTIs with the corner fractional charge adjustable within the range $(0, 1)$, based on the 2D SSH model lattice and the Lorentz transformation. The four-fold degenerate corner states in the undeformed 2D SSH model lattice get reduced to two pairs of two-fold degenerate corner states after the transformation. Notably, we also have observed BIC-like localized corner states in the deformed lattice (even though it

remains in a topological trivial phase), which are absent in the undeformed lattice. These results not only present a novel method for achieving light-beam localization, but also offer deeper insights into the fractional charge associated with the corner states. Our results also possess considerable potential for applications in preparing high-quality cavities [34], and may inspire new ideas in producing compact optical functional devices [53].

References:

- [1] T. Ozawa, H. M. Price, A. Amo, N. Goldman, M. Hafezi, L. Lu, M. C. Rechtsman, D. Schuster, J. Simon, O. Zilberberg, and I. Carusotto, “Topological photonics,” *Reviews of Modern Physics*, vol. 91, no. 1, pp. 15006, 2019.
- [2] D. Smirnova, D. Leykam, Y. Chong, and Y. Kivshar, “Nonlinear topological photonics,” *Applied Physics Reviews*, vol. 7, no. 2, pp. 021306, 2020.
- [3] B. Xie, H. X. Wang, X. Zhang, P. Zhan, J. H. Jiang, M. Lu, and Y. Chen, “Higher-order band topology,” *Nature Reviews Physics*, vol. 3, no. 7, pp. 520-532, 2021.
- [4] X. Zhang, F. Zangeneh-Nejad, Z. G. Chen, M. H. Lu, and J. Christensen, “A second wave of topological phenomena in photonics and acoustics,” *Nature*, vol. 618, no. 7966, pp. 687-697, 2023.
- [5] Z. K. Lin, Q. Wang, Y. Liu, H. Xue, B. Zhang, Y. Chong, and J. H. Jiang, “Topological phenomena at defects in acoustic, photonic and solid-state lattices,” *Nature Reviews Physics*, vol. 5, no. 8, pp. 483-495, 2023.
- [6] W. A. Benalcazar, B. A. Bernevig, and T. L. Hughes, “Quantized electric multipole insulators,” *Science*, vol. 357, no. 6346, pp. 61-66, 2017.
- [7] M. Serra-Garcia, V. Peri, R. Süsstrunk, O. R. Bilal, T. Larsen, L. G. Villanueva, and S. D. Huber, “Observation of a phononic quadrupole topological insulator,” *Nature*, vol. 555, no. 7696, pp. 342-345, 2018.
- [8] X. Ni, M. Li, M. Weiner, A. Alù, and A. B. Khanikaev, “Demonstration of a quantized acoustic octupole topological insulator,” *Nature Communications*, vol. 11, no. 1, pp. 2108, 2020.
- [9] H. Xue, Y. Ge, H. X. Sun, Q. Wang, D. Jia, Y. J. Guan, S. Q. Yuan, Y. Chong, and B. Zhang, “Observation of an acoustic octupole topological insulator,” *Nature Communications*, vol. 11, no. 1, pp. 2442, 2020.
- [10] J. Li, Q. Mo, J. H. Jiang, and Z. Yang, “Higher-order topological phase in an acoustic fractal lattice,” *Science Bulletin*, vol. 67, no. 20, pp. 2040-2044, 2022.
- [11] J. Schulz, J. Noh, W. A. Benalcazar, G. Bahl, and G. von Freymann, “Photonic quadrupole topological insulator using orbital-induced synthetic flux,” *Nature Communications*, vol. 13, no. 1, pp. 6597, 2022.
- [12] W. A. Benalcazar, T. Li, and T. L. Hughes, “Quantization of fractional corner charge in C_n -symmetric higher-order topological crystalline insulators,” *Physical Review B*, vol. 99, no. 24, pp. 245151, 2019.
- [13] B. Y. Xie, H. F. Wang, H. X. Wang, X. Y. Zhu, J. H. Jiang, M. H. Lu, and Y. F. Chen, “Second-order photonic topological insulator with corner states,” *Physical Review B*, vol. 98, no. 20, pp. 205147, 2018.
- [14] J. Noh, W. A. Benalcazar, S. Huang, M. J. Collins, K. P. Chen, T. L. Hughes, and M. C. Rechtsman, “Topological protection of photonic mid-gap defect modes,” *Nature Photonics*, vol. 12, no. 7, pp. 408-415, 2018.
- [15] B. Y. Xie, G. X. Su, H. F. Wang, H. Su, X. P. Shen, P. Zhan, M. H. Lu, Z. L. Wang, and Y. F. Chen, “Visualization of higher-order topological insulating phases in two-dimensional dielectric photonic crystals,” *Physical Review Letters*, vol. 122, no. 23, pp. 233903, 2019.
- [16] X. D. Chen, W. M. Deng, F. L. Shi, F. L. Zhao, M. Chen, and J. W. Dong, “Direct observation of corner states in second-order topological photonic crystal slabs,” *Physical Review Letters*, vol. 122, no. 23, pp. 233902, 2019.
- [17] A. El Hassan, F. K. Kunst, A. Moritz, G. Andler, E. J. Bergholtz, and M. Bourennane, “Corner states of light in photonic waveguides,” *Nature Photonics*, vol. 13, no. 10, pp. 697-700, 2019.
- [18] X. Ni, M. Weiner, A. Alù, and A. B. Khanikaev, “Observation of higher-order topological acoustic states protected by generalized chiral symmetry,” *Nature Materials*, vol. 18, no. 2, pp. 113-120, 2019.
- [19] H. Xue, Y. Yang, F. Gao, Y. Chong, and B. Zhang, “Acoustic higher-order topological insulator on a kagome lattice,” *Nature Materials*, vol. 18, no. 2, pp. 108-112, 2019.
- [20] M. Li, D. Zhirihin, M. Gorbach, X. Ni, D. Filonov, A. Slobozhanyuk, A. Alù, and A. B. Khanikaev, “Higher-order topological states in photonic

- kagome crystals with long-range interactions,” *Nature Photonics*, vol. 14, no. 2, pp. 89-94, 2020.
- [21] Y. Zhang, Y. V. Kartashov, L. Torner, Y. Li, and A. Ferrando, “Nonlinear higher-order polariton topological insulator,” *Optics Letters*, vol. 45, no. 17, pp. 4710-4713, 2020.
- [22] M. S. Kirsch, Y. Zhang, M. Kremer, L. J. Maczewsky, S. K. Ivanov, Y. V. Kartashov, L. Torner, D. Bauer, A. Szameit, and M. Heinrich, “Nonlinear second-order photonic topological insulators,” *Nature Physics*, vol. 17, no. 9, pp. 995-1000, 2021.
- [23] S. Zheng, X. Man, Z. L. Kong, Z. K. Lin, G. Duan, N. Chen, D. Yu, J. H. Jiang, and B. Xia, “Observation of fractal higher-order topological states in acoustic metamaterials,” *Science Bulletin*, vol. 67, no. 20, pp. 2069-2075, 2022.
- [24] B. Ren, A. A. Arkhipova, Y. Zhang, Y. V. Kartashov, H. Wang, S. A. Zhuravitskii, N. N. Skryabin, I. V. Dyakonov, A. A. Kalinkin, S. P. Kulik, V. O. Kompanets, S. V. Chekalin, and V. N. Zadkov, “Observation of nonlinear disclination states,” *Light: Science and Applications*, vol. 12, no. 1, pp. 194, 2023.
- [25] A. A. Arkhipova, Y. Zhang, Y. V. Kartashov, S. A. Zhuravitskii, N. N. Skryabin, I. V. Dyakonov, A. A. Kalinkin, S. P. Kulik, V. O. Kompanets, S. V. Chekalin, and V. N. Zadkov, “Observation of π solitons in oscillating waveguide arrays,” *Science Bulletin*, vol. 68, no. 18, pp. 2017-2024, 2023.
- [26] H. Zhong, V. O. Kompanets, Y. Zhang, Y. V. Kartashov, M. Cao, Y. Li, S. A. Zhuravitskii, N. N. Skryabin, I. V. Dyakonov, A. A. Kalinkin, S. P. Kulik, S. V. Chekalin, and V. N. Zadkov, “Observation of nonlinear fractal higher order topological insulator,” *Light: Science and Applications*, vol. 13, no. 1, pp. 264, 2024.
- [27] L. He, Z. Addison, E. J. Mele, and B. Zhen, “Quadrupole topological photonic crystals,” *Nature Communications*, vol. 11, no. 1, pp. 3119, 2020.
- [28] G. Cáceres-Aravena, M. Nedić, P. Vildoso, G. Gligorić, J. Petrovic, A. Maluckov, and R. A. Vicencio, “Compact topological edge states in flux-dressed graphenelike photonic lattices,” *Physical Review Letters*, vol. 133, no. 11, pp. 116304, 2024.
- [29] C. W. Peterson, T. Li, W. Jiang, T. L. Hughes, and G. Bahl, “Trapped fractional charges at bulk defects in topological insulators,” *Nature*, vol. 589, no. 7842, pp. 376-380, 2021.
- [30] Y. Liu, S. Leung, F. F. Li, Z. K. Lin, X. Tao, Y. Poo, and J. H. Jiang, “Bulk-disclination correspondence in topological crystalline insulators,” *Nature*, vol. 589, no. 7842, pp. 381-385, 2021.
- [31] S. Wu, B. Jiang, Y. Liu, and J. H. Jiang, “All-dielectric photonic crystal with unconventional higher-order topology,” *Photonics Research*, vol. 9, no. 5, pp. 668-677, 2021.
- [32] H. X. Wang, L. Liang, B. Jiang, J. Hu, X. Lu, and J. H. Jiang, “Higher-order topological phases in tunable C_3 symmetric photonic crystals,” *Photonics Research*, vol. 9, no. 9, pp. 1854-1864, 2021.
- [33] C. Shang, S. Liu, C. Jiang, R. Shao, X. Zang, C. H. Lee, R. Thomale, A. Manchon, T. J. Cui, and U. Schwingenschlögl, “Observation of a higher-order end topological insulator in a real projective lattice,” *Advanced Science*, vol. 11, no. 11, pp. 2303222, 2024.
- [34] Y. Ota, F. Liu, R. Katsumi, K. Watanabe, K. Wakabayashi, Y. Arakawa, and S. Iwamoto, “Photonic crystal nanocavity based on a topological corner state,” *Optica*, vol. 6, no. 6, pp. 786-789, 2019.
- [35] S. Mittal, V. V. Orre, G. Zhu, M. A. Gorlach, A. Poddubny, and M. Hafezi, “Photonic quadrupole topological phases,” *Nature Photonics*, vol. 13, no. 10, pp. 692-696, 2019.
- [36] J. D. Jackson, *Classical Electrodynamics*, 3rd edition. Hoboken, New Jersey, USA: John Wiley & Sons, Ltd, 1998, pp. 514-578.
- [37] M. C. Rechtsman, J. M. Zeuner, Y. Plotnik, Y. Lumer, D. Podolsky, F. Dreisow, S. Nolte, M. Segev, and A. Szameit, “Photonic Floquet topological insulators,” *Nature*, vol. 496, no. 7444, pp. 196-200, 2013.
- [38] S. Mukherjee, A. Spracklen, M. Valiente, E. Andersson, P. Öhberg, N. Goldman, and R. R. Thomson, “Experimental observation of anomalous topological edge modes in a slowly driven photonic lattice,” *Nature Communications*, vol. 8, no. 1, pp. 13918, 2017.
- [39] L. J. Maczewsky, J. M. Zeuner, S. Nolte, and A. Szameit, “Observation of photonic anomalous Floquet topological insulators,” *Nature Communications*, vol. 8, no. 1, pp. 13756, 2017.
- [40] X. Zhang, H. X. Wang, Z. K. Lin, Y. Tian, B. Xie, M. H. Lu, Y. F. Chen, and J. H. Jiang, “Second-order topology and multidimensional topological transitions in sonic crystals,” *Nature Physics*, vol. 15, no. 6, pp. 582-588, 2019.
- [41] S. Mukherjee and M. C. Rechtsman, “Observation of Floquet solitons in a topological bandgap,” *Science*, vol. 368, no. 6493, pp. 856-859, 2020.
- [42] L. J. Maczewsky, M. Heinrich, M. Kremer, S. K. Ivanov, M. Ehrhardt, F. Martinez, Y. V. Kartashov, V. V. Konotop, L. Torner, D. Bauer, and

- A. Szameit, “Nonlinearity-induced photonic topological insulator,” *Science*, vol. 370, no. 6517, pp. 701-704, 2020.
- [43] Y. V. Kartashov, A. A. Arkhipova, S. A. Zhuravitskii, N. N. Skryabin, I. V. Dyakonov, A. A. Kalinkin, S. P. Kulik, V. O. Kompanets, S. V. Chekalin, L. Torner, and V. N. Zadkov, “Observation of edge solitons in topological trimer arrays,” *Physical Review Letters*, vol. 128, no. 9, pp. 093901, 2022.
- [44] P. Wang, Y. Zheng, X. Chen, C. Huang, Y. V. Kartashov, L. Torner, V. V. Konotop, and F. Ye, “Localization and delocalization of light in photonic moiré lattices,” *Nature*, vol. 577, no. 7788, pp. 42-46, 2020.
- [45] Q. Fu, P. Wang, C. Huang, Y. V. Kartashov, L. Torner, V. V. Konotop, and F. Ye, “Optical soliton formation controlled by angle twisting in photonic moiré lattices,” *Nature Photonics*, vol. 14, no. 11, pp. 663-668, 2020.
- [46] H. Zhong, S. Xia, Y. Zhang, Y. Li, D. Song, C. Liu, and Z. Chen, “Nonlinear topological valley Hall edge states arising from type-II Dirac cones,” *Advanced Photonics*, vol. 3, no. 5, pp. 56001, 2021.
- [47] Z. Hu, D. Bongiovanni, D. Jukić, E. Jajtić, S. Xia, D. Song, J. Xu, R. Morandotti, H. Buljan, and Z. Chen, “Nonlinear control of photonic higher-order topological bound states in the continuum,” *Light: Science and Applications*, vol. 10, no. 1, pp. 164, 2021.
- [48] Y. Zhang, D. Bongiovanni, Z. Wang, X. Wang, S. Xia, Z. Hu, D. Song, D. Jukić, J. Xu, R. Morandotti, H. Buljan, and Z. Chen, “Realization of photonic p -orbital higher-order topological insulators,” *eLight*, vol. 3, no. 1, pp. 5, 2023.
- [49] G. Jotzu, M. Messer, R. Desbuquois, M. Lebrat, T. Uehlinger, D. Greif, and T. Esslinger, “Experimental realisation of the topological Haldane model,” *Nature*, vol. 515, no. 7526, pp. 237-240, 2014.
- [50] Z. Y. Zhang, R. Wang, Y. Q. Zhang, Y. V. Kartashov, F. Li, H. Zhong, H. Guan, K. Gao, F. L. Li, Y. P. Zhang, and M. Xiao, “Observation of edge solitons in photonic graphene,” *Nature Communications*, vol. 11, no. 1, pp. 1902, 2020.
- [51] Y. Q. Zhang, M. R. Belić, H. B. Zheng, Z. K. Wu, Y. Y. Li, K. Q. Lu, and Y. P. Zhang, “Fresnel diffraction patterns as accelerating beams,” *Europhysics Letters (EPL)*, vol. 104, no. 3, pp. 34007, 2013.
- [52] S. K. Ivanov, Y. V. Kartashov, and L. Torner, “Light bullets in Su-Schrieffer-Heeger photonic

topological insulators,” *Physical Review A*, vol. 107, no. 3, pp. 33514, 2023.

- [53] C. C. Lu, H. Y. Yuan, H. Y. Zhang, W. Zhao, N. E. Zhang, Y. J. Zheng, S. Elshahat, and Y. C. Liu, “On-chip topological nanophotonic devices,” *Chip*, vol. 1, no. 4, pp. 100025, 2022.



Yuwei Hu is currently a master student of School of Electronic Science and Engineering, Xi’an Jiaotong University, Xi’an, China. He received the B. S. degree from Henan Polytechnic University, Jiaozuo, China in 2022. His research interest is topological photonics.



Suge Feng is currently a master student of School of Electronic Science and Engineering, Xi’an Jiaotong University, Xi’an, China. She received the B. S. degree from Nanjing Normal University, Nanjing, China in 2022. Her research interest is high-order topological insulators.



Boquan Ren is currently a Ph.D. student of School of Electronic Science and Engineering, Xi’an Jiaotong University, Xi’an, China. She received the B. S. degree and the M. S. degree from Xi’an Polytechnic University, Xi’an, China in 2017 and 2020, respectively. Her research interest is the topological photonics.

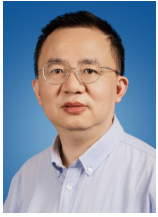


Hua Zhong is currently an Assistant Professor of School of Electronic Science and Engineering, Xi’an Jiaotong University, Xi’an, China. She received the B. S. degree from Qingdao University of Technology, Qingdao, China in 2015. She received the M. S. degree and the Ph. D. from Xi’an Jiaotong University, Xi’an, China in 2018 and 2022, respectively. Her interest is topological photonics.



Milivoj R. Belić obtained B. S. degree in physics from University of Belgrade in 1974, and Ph. D. from City College of New York in 1980. Currently, he is Professor of Hamad Bin Khalifa University in Qatar. Dr. Belić’s research includes nonlinear optics and dynamics. He coauthored 6 books and more than 800 papers that attracted over 24000 citations; his h-index is 70. Dr. Belić received many research awards, including Galileo Galilei Medal from International Commission for Optics and Research Team Award from QNRF. He is Senior Member of

Optica and Member of Serbian Academy of Nonlinear Sciences.



Meng Cao is currently a Professor of School of Electronic Science and Engineering, Xi'an Jiaotong University, Xi'an, China. He received the M. S. degree and the Ph. D. from Xi'an Jiaotong University, Xi'an, China in 2001 and 2006, respectively. His research interests include electron beam-material interactions, Monte Carlo simulation for vacuum electronic devices.



Yongdong Li was born in Hunan, China, in 1974. He received the B. S. degree, the M. S. degree and the Ph. D. from Xi'an Jiaotong University, Xi'an, China in 1996, 2000, and 2005, respectively. He is now a Professor of School of Electronic Science and Engineering, Xi'an Jiaotong

University, Xi'an, China. His research interests include beam-microwave interactions, particle-in-cell method for vacuum electronic devices and gas discharges.



Yiqi Zhang is currently a Professor of School of Electronic Science and Engineering, Xi'an Jiaotong University, Xi'an, China. He received the B. S. degree from Tianjin University, Tianjin, China in 2006 and the Ph. D. from Xi'an Institute of Optics and Precision Mechanics of Chinese Academy of Sciences, Xi'an, China in 2011. His research interest mainly focuses on the nonlinear manipulation of topological light fields in photonic lattices. Being the first author as well as the corresponding author, he has published more than 90 SCI-indexed papers in peer reviewed journals, including *Nature Physics*, *Nature Communications*, *Light: Science and Applications*, *Physical Review Letters*, *Advanced Photonics*, *Science Bulletin*.